

DISCOVERY OF A RADIO SUPERNOVA REMNANT AND NON-THERMAL X-RAYS COINCIDENT WITH THE TEV SOURCE HESS J1813–178

C. L. BROGAN¹, B. M. GAENSLER², J. D. GELFAND², J. S. LAZENDIC³, T. J. LAZIO⁴, N. E. KASSIM⁴, N. M. MCCLURE-GRIFFITHS⁵

Draft version May 24, 2019

ABSTRACT

We present the discovery of non-thermal radio and X-ray emission positionally coincident with the TeV γ -ray source HESS J1813–178. We demonstrate that the non-thermal radio emission is due to a young shell-type supernova remnant (SNR) G12.8–0.0, and constrain its distance to be greater than 4 kpc. The non-thermal X-ray emission is consistent with originating from the SNR shell or an unidentified pulsar/pulsar wind nebula; pulsed emission is not detected in archival *ASCA* data. The X-ray emission falls on a direct extrapolation of the radio synchrotron power-law before the roll-off due to radiative losses, an unusual occurrence and remarkable coincidence if the origin of the emission is not the same (i.e. the SNR shell). Assuming that the radio and X-ray emission originate from the SNR shell we find that G12.8–0.0 accelerates electrons up to at least 450 TeV, higher than for any other SNR yet observed. A model that incorporates data spanning 18 decades in frequency suggests that inverse Compton emission off the cosmic microwave background cannot account for the TeV emission. Further observations are needed to confirm that the broadband emission has a common origin.

Subject headings: acceleration of particles – supernova remnants – radio:ISM – Xrays:ISM – ISM: individual (G12.8-0.0, HESS J1813-178)

1. INTRODUCTION

Based on theoretical arguments, it has become widely accepted that a significant fraction of Galactic cosmic rays with energies $> 10^{15}$ eV are generated in shell type supernova remnants (SNRs) (e.g. Blandford & Eichler 1987). While the detection of non-thermal X-rays from the shells of several SNRs provides evidence that SNR shocks are efficient accelerators of $> 10^{13}$ eV electrons (see e.g. Reynolds 1996), direct evidence is still lacking that (i) SNRs can accelerate particles all the way up to the “knee” in the cosmic ray spectrum at 10^{15} eV, and (ii) SNRs efficiently accelerate protons and heavy nuclei as well as electrons (see Pohl 2001, for a review). Powerful constraints on shock acceleration in SNRs can come from the detection of TeV γ -rays. However, these very high energy photons can be produced by a variety of mechanisms, including inverse Compton (IC) emission from energetic electrons, and pion decay produced by the collision of energetic protons with surrounding dense gas. Several other types of energetic Galactic sources have also been suggested as TeV γ -ray counterparts including pulsars, pulsar wind nebulae (PWN), microquasars, and massive star forming regions. Multiwavelength data and careful modeling are thus needed to identify these elusive sources and infer the properties of Galactic cosmic ray acceleration (Pohl 2001).

Currently only one convincing shell SNR/TeV association is known (SNR G347.3–0.5; Aharonian et al. 2004, and reference therein), and observations do not yet unambiguously distinguish between hadronic and leptonic acceleration (Lazendic et al. 2004; Malkov, Diamond, & Sagdeev 2005).

However, with the advent of a number of new sensitive Čerenkov imaging telescopes, there are bright prospects for discovering additional TeV sources. Indeed, Aharonian et al. (2005a) recently reported the discovery of eight new high energy γ -ray sources ($E > 10^{11}$ eV) in the inner Galactic plane ($-30^\circ < \ell < 30^\circ$) using the High Energy Stereoscopic System (HESS). Of the eight new TeV sources, six are listed in Aharonian et al. (2005a) as being in close proximity to either an SNR, pulsar, or *EGRET* source (in some cases all three). However, these authors were unable to identify any plausible counterparts to two of the new TeV sources and suggest that they may represent a new class of “dark” nucleonic particle accelerators.

In this *Letter* we present evidence that one of the two “dark” TeV sources, HESS J1813–178, is positionally coincident with a previously unidentified young radio and X-ray SNR, G12.8–0.0. The spectrum of G12.8–0.0 is consistent with an unbroken power-law spectrum over at least 10 decades of frequency, from 330 MHz up to at least 10 keV, indicating that it is an efficient accelerator of energetic electrons. We model the TeV emission observed by HESS in the context of this radio and X-ray emission, and conclude that if all the flux has a common origin, IC emission from the cosmic microwave background cannot account for the observed TeV photons.

2. DATA AND RESULTS

2.1. The Radio Source G12.82–0.02

The radio source G12.82–0.02 was discovered in a new low frequency Very Large Array (VLA) 90cm survey incorporating B+C+D configuration data (Brogan et al. 2005). The previously unidentified radio source has a shell morphology with a diameter of 2.5° . Subsequent analysis of archival VLA C+D configuration 20cm data has confirmed this discovery, and indicates that the radio emission is non-thermal. G12.82–0.02 has integrated radio flux densities at 20 and 90 cm of 0.65 ± 0.1 and 1.2 ± 0.08 Jy, respectively. Figure 1a shows the 90cm discovery image while Figure 1b shows a 3-color image of the region using 90cm, 20cm, and 8 μ m *Spitzer Space Telescope* GLIMPSE data (Benjamin et al. 2003). It is notable

arXiv:astro-ph/0505145v1 7 May 2005

¹ Institute for Astronomy, 640 North A‘ohoku Place, Hilo, HI 96720; cbrogan@ifa.hawaii.edu.

² Harvard-Smithsonian Center for Astrophysics, 60 Garden Street, Cambridge, MA 02138

³ MIT Kavli Institute for Astrophysics and Space Research, Cambridge MA 02319

⁴ Remote Sensing Division, Naval Research Laboratory, Washington DC 20375-5351

⁵ Australia Telescope National Facility, CSIRO, P.O. Box 76, Epping, NSW 1710, Australia

that no distinct (non-diffuse) dust emission is coincident with G12.82–0.02, confirming its non-thermal nature. The radio and TeV sources are located $\sim 8^\circ$ from the H II region complex W33 (see Fig. 1a,b, §3.1). The TeV source HESS J1813–178 (positional uncertainty $1^0\text{--}2^0$) is coincident with the radio shell (see Fig. 1a). The best fit size for HESS J1813–178 is 3^0 , in excellent agreement with the that of G12.82–0.02; no structure is evident in the published 3^0 resolution HESS image (Aharonian et al. 2005a).

Although not previously recognized as a distinct source, G12.82–0.02 does appear as a faint unresolved extension to W33 in the Nobeyama 3cm, Parkes 6cm, and Bonn 11cm surveys, with resolutions ranging from 3^0 to 4.3^0 (Haynes et al. 1978; Handa et al. 1987; Reich, Reich, & Fuerst 1990). The radio spectrum of G12.82–0.02 (including the 20 and 90cm VLA data, 4m VLA B+C+D configuration data from Brogan et al. (2004), and the single dish data) is displayed in Figure 1c. The rms noise in the 20 and 90cm images are 5 and 2.5 mJy beam $^{-1}$, respectively, and the flux density uncertainty is $(\# \text{ independent beams})^{0.5} \sim 3$. G12.82–0.02 is not detected at 4m, and the flux density shown in Figure 1c is a 5 μ Jy upper limit (also see §3.1). To account for the extra uncertainty due to confusion with W33, 6 μ Jy was used for the single dish uncertainties. The spectral index using these data (excluding the 4m non-detection) and a weighted least squares fit is -0.48 ± 0.03 (assumes $S \propto \nu^{-\alpha}$). If only the more reliable 20 and 90cm data are used the spectral index is flatter: -0.42 ± 0.03 . Assuming $\alpha = -0.48$, the 1 GHz surface brightness of G12.82–0.02 is $1_{\text{GHz}} \sim 3.3 \times 10^{-20} \text{ W m}^{-2} \text{ Hz sr}^{-1}$, and the radio luminosity from $10^7\text{--}10^{11} \text{ Hz}$ is $3.6(d=d_4)^2 \times 10^{32} \text{ ergs s}^{-1}$ (d is the distance and $d_4 = 4 \text{ kpc}$; see §3.1). The radio morphology, radio spectrum, and lack of coincident mid-infrared emission (Fig. 1) provide convincing evidence that G12.82–0.02 is a previously unidentified shell type SNR; henceforth designated SNR G12.8–0.0.

2.2. The X-ray Source AX J1813–178

Analysis of a pointed 20 ks archival *ASCA* observation toward this region (taken in 1997 September) reveals a source, hereafter AX J1813–178, spatially coincident with both SNR G12.8–0.0 and HESS J1813–178. AX J1813–178 is detected by all four *ASCA* instruments (SIS0, SIS1, GIS2, and GIS3), although the emission is contaminated in the GIS detectors by the bright X-ray binary GX 13+1 $\sim 40^\circ$ to the NE. Thus, we have confined our spectral and imaging analysis to the SIS data. A close-up view of the X-ray and radio emission is shown in Figure 2. The X-ray source appears to be either unresolved or only slightly extended. The peak of the X-rays nominally lies interior to the radio shell, but since the *ASCA* pointing uncertainty can be as large as 1^0 (Gotthelf et al. 2000), the *ASCA* image does not distinguish between X-rays originating from the center or the rim of the shell.

The background-corrected SIS data consist of ~ 2000 counts in the energy range 0.5–10 keV, which we fit jointly to three absorbed spectral models: (1) a power-law, (2) a blackbody, and (3) a Raymond-Smith (RS) thermal plasma (with and without the abundances frozen at solar). In a statistical sense, all three models give good fits to the data (reduced $\chi^2 \sim 1$). However, the RS model yields an unrealistically high temperature for the shocked gas in a SNR ($\sim 80 \text{ keV}$), while the blackbody fit implies a substantially higher temperature ($kT \sim 1.7 \text{ keV}$) and smaller emitting area (equivalent radius $\sim 0.1 \text{ km}$ at a distance of 4 kpc) than is seen for neu-

tron stars or their polar caps (e.g., Kaspi et al. 2005). Thus, the power-law fit is the most physically plausible and yields an absorbing column $N_H = (1.1 \pm 0.2) \times 10^{23} \text{ cm}^{-2}$, a spectral index $\alpha = -0.8 \pm 0.4$ and an unabsorbed flux (2–10 keV) of $7.0 \times 10^{-12} \text{ ergs cm}^{-2} \text{ s}^{-1}$. The 2–10 keV unabsorbed luminosity of AX J1813–178 is $1.7(d=d_4)^2 \times 10^{34} \text{ ergs s}^{-1}$.

3. DISCUSSION

3.1. Distance Constraints

As mentioned previously, SNR G12.8–0.0 lies in close proximity to the W33 H II region/active star formation complex. The free-free emission (radio recombination lines), molecular line (including masers), and H I gas associated with W33 arise from velocity components at 30 and 50 km s $^{-1}$; the latter is more prominent on the western side of the complex (e.g. Sato 1977; Bieging et al. 1978; Gardner et al. 1983). No H I absorption features are evident toward W33 beyond 55 km s $^{-1}$ (Radhakrishnan et al. 1972). Since the tangent point velocity is 170 km s $^{-1}$ in this direction (assumes Galactic center distance 8.5 kpc and rotation curve from Fich et al. 1989), W33 must lie at about the 55 km s $^{-1}$ near distance of 4.3 kpc. H I absorption spectra from the Southern Galactic Plane Survey (SGPS) (resolution 1^0 , see McClure-Griffiths et al. 2005) show that similar to W33, the H I spectrum toward SNR G12.8–0.0 shows absorption to, but not beyond 55 km s $^{-1}$, although the signal-to-noise is low toward this weak source. Thus, the distance to G12.8–0.0 is likely to be $\sim 4 \text{ kpc}$.

Based on the derived spectral index (-0.42 to -0.48) the expected 4m flux density is 2.3 to 2.5 Jy, suggesting that SNR G12.8–0.0 should be readily detectable, yet it is not (Fig. 1c, §2.1). This discrepancy could be due to the close proximity of W33 if G12.8–0.0 lies immersed in or behind the H II region due to free-free absorption. Indeed, free-free absorption by H II regions is thought to contribute to the large number of Galactic SNRs with low frequency spectral turnovers (Kassim 1989). In interferometric low frequency images Galactic H II regions can appear in absorption against the resolved out diffuse Galactic plane synchrotron emission. The VLA 4m image shows that W33 H II region is coincident with such a 4m absorption ‘hole’, and its extent matches that of the diffuse 90cm and 8 m emission associated with W33 (Fig. 1b). The emission/absorption at all three wavelengths extends as far west as SNR G12.8–0.0. Thus, free-free absorption is the most natural explanation for the non-detection of G12.8–0.0 at 4m, and confirms the H I result that the SNR must lie at the distance of or behind W33.

The very high column density derived from the *ASCA* data, $N_H \sim 10^{23} \text{ cm}^{-2}$, also suggests that SNR G12.8–0.0 lies behind W33. Along nearby lines of sight, the total H I column density integrated through the Galaxy is $\sim 2 \times 10^{22} \text{ cm}^{-2}$ (Dickey & Lockman 1990), so clearly a significant discrete source of absorption must be in the foreground to the SNR. CO data (Dame et al. 2001) indicate that dense gas in the distance range 0–4 kpc (much of which is almost certainly associated with W33) contributes a hydrogen column density $\sim 8 \times 10^{22} \text{ cm}^{-2}$, and can thus account for much for the X-ray absorption. This further argues for a distance 4 kpc or greater for SNR G12.8–0.0 in agreement with independent estimates from H I and free-free absorption; we adopt a fiducial minimum distance of 4 kpc (d_4) for the remaining discussion.

3.2. The Probable Youth of SNR G12.8–0.0

The small angular size of SNR G12.8–0.0 (2.5°) suggests that it is quite young; certainly the high extinction toward this region would have prevented its detection optically. The radius of SNR G12.8–0.0 is $1.5(d=d_4)$ pc. If the SNR is still freely expanding at a speed V_5 , its age is $285(d=d_4)(V=V_5)^{-1}$ years ($V_5 = 5;000$ km s $^{-1}$). If the distance is 4–10 kpc, use of the free-expansion age is justified since the swept up mass is still a small fraction of the ejected mass at the corresponding radii. If the distance to SNR G12.8–0.0 is significantly greater, the SNR is likely to have made the transition to the Sedov-Taylor phase (Sedov 1959). For example, on the far side of the Galaxy at 20 kpc, the swept up mass is 50 M $_{\odot}$ (assuming an ambient density $n_o = 1$ cm $^{-3}$ and 10% helium abundance) and the Sedov-Taylor age is $2;520(n_o)^{0.5}(E=E_{51})^{-0.5}$ years (where E is the kinetic energy of the explosion and $E_{51} = 10^{51}$ ergs). Thus, independent of distance, if SNR G12.8–0.0 is expanding into a typical density medium it is very young with representative age estimates in the range 285–2,500 years. Excluding G12.8–0.0, only six shell type Galactic SNRs with diameters $\leq 3^\circ$ are currently known, undoubtedly due to observational selection effects since an order of magnitude more are expected (Green 2004). Our discovery highlights the potential effectiveness of high resolution and sensitivity low radio frequency surveys in finding young Galactic SNRs.

3.3. TeV Emission from a Young Pulsar?

Although there is excellent positional agreement between the radio, X-ray, and TeV emission (Fig. 2), it is currently unclear whether all these components originate from the SNR shell or if there is an as yet unidentified associated pulsar or PWN. No central radio nebula or point source is detected at our current spatial resolution and sensitivity, and there are no known radio pulsars in or near the SNR in the catalog of Manchester et al. (2005). This field has been searched for pulsars as part of the Parkes multi-beam pulsar survey, down to a limiting 1.4 GHz flux density of 0.2 mJy (Manchester et al. 2001), corresponding to a pseudoluminosity of $3(d=d_4)^2$ mJy kpc 2 . Recent deep pulsar searches toward SNRs have been able to either detect or place upper limits of ≤ 1 mJy kpc 2 on the 1.4 GHz pseudoluminosity of central pulsars (e.g. Camilo et al. 2002). Thus, the Parkes multi-beam survey is reasonably constraining, but a deeper search is clearly needed.

The X-ray luminosity and spectral index inferred in §2.2 for AX J1813–178 are typical of young pulsars and their associated PWN (e.g. Possenti et al. 2002). In order to search for X-ray pulsations from AX J1813–178 we conducted a Z_n^2 search (see Buccheri et al. 1983) on the barycenter-corrected ASCA high-bit mode GIS data. No pulsed signal was seen for harmonics $n = 1;2;3;4$ from 585 counts selected between 4–8 keV. For periods between 125 ms and 1000 s, we find an upper limit on the pulsed fraction of 38% (19%) for a sinusoidal (sharply peaked) pulse profile. Since most young pulsars rotate with periods below this range, and the pulsed signal may be a small fraction ($< 10\%$) of the total pulsar plus PWN X-ray flux, the lack of pulsations is both unsurprising and unconstraining. While further X-ray and radio observations are clearly needed to confirm or rule out a pulsar/PWN interpretation for AX J1813–178, we note from Figure 3 (to be discussed further in §3.4) that the X-ray emission lies almost exactly on the extrapolation of the radio synchrotron spectrum, without any need for a spectral break or roll-over. It would

thus be a remarkable coincidence if the X-rays were from a pulsar/PWN, when the radio emission is so clearly from a SNR shell. We thus favor the interpretation that the non-thermal X-rays and TeV emission are not from a neutron star or its nebula, but originate from the shell of SNR G12.8–0.0. We next consider this possibility.

3.4. TeV Emission from the SNR Shell?

Aharonian et al. (2005a) distinguish between a counterpart and simple positional agreement; a counterpart must also have a plausible TeV emission mechanism. An SNR presents multiple possibilities for the γ -ray emission mechanism. For example, photons from the cosmic microwave background (CMB) could scatter off shock accelerated electrons in the SNR to produce IC emission or the electrons themselves could be accelerated to high enough energies to produce nonthermal bremsstrahlung. If the SNR were immersed in dense molecular gas, the decay of pions from accelerated nuclei could also produce the TeV emission.

Assuming that the radio, X-ray, and TeV emission originate from the SNR shell, we have modeled the flux expected from from synchrotron+IC mechanisms. Since the TeV spectrum has not yet been published, we fit the radio and X-ray data using a power law energy distribution modified by an exponential cutoff $dN=dE E^{-\alpha} \exp[-(E=E_{max})]$, where α is the index of the electron distribution, and E_{max} is the maximum energy of accelerated particles (see Lazendic et al. 2004, for more details). The multiwavelength data and model fit are shown in Figure 3, and our model parameters are described in the caption.

Remarkably, the X-ray data lies on the extrapolated synchrotron curve before the roll-off due to radiative losses; this is the first such case observed in SNRs (see e.g. Reynolds & Keohane 1999). This means that we can only derive a lower limit to E_{max} ; we infer $E_{max} \gtrsim 450$ TeV, higher than any E_{max} yet found for an SNR (Reynolds & Keohane 1999; Hendrick & Reynolds 2001). Even if we have underestimated the assumed magnetic field strength ($B = 10$ G) by an order of magnitude, E_{max} is still greater than 150 TeV. Interestingly, the modeled IC spectrum falls well below the HESS data assuming only CMB scattering. Thus, our preliminary results raise the possibility that the TeV emission is the signature of accelerated nuclei and hence pion decay (e.g. Uchiyama et al. 2005). It is also possible that a more sophisticated IC model incorporating, for example, scattering off starlight (Aharonian et al. 2005b) could better accommodate the HESS data. Detection of resolved X-ray and TeV emission from the SNR shell would strengthen our suggestions that the radio, X-ray, and TeV emission have the same origin and that interaction of SNR G12.8–0.0 with dense ambient material (possibly associated with W33) is responsible for the TeV emission.

Basic research in radio astronomy at the Naval Research Laboratory is supported by the Office of Naval Research. The VLA is operated by the National Radio Astronomy Observatory which is a facility of the National Science Foundation operated under cooperative agreement by Associated Universities, Inc. This research has made use of the High Energy Astrophysics Science Archive Research Center (HEASARC), provided by NASA's Goddard Space Flight Center.

REFERENCES

- Aharonian, F., et al. 2005a, *Science*, 307, 1938
 Aharonian, F., et al. 2005b, *A&A*, 432, L25
 Aharonian, F. A., et al. 2004, *Nature*, 432, 75
 Benjamin, R. A., et al. 2003, *PASP*, 115, 953
 Bieging, J. H., Pankonin, V., & Smith, L. F. 1978, *A&A*, 64, 341
 Blandford, R., & Eichler, D. 1987, *Phys. Rep.*, 154, 1
 Brogan, C. L., et al. 2004, *AJ*, 127, 355
 Brogan, C. L., Gelfand, J. D., Gaensler, B. M., Kassim, N. E., & Lazio, T. J., 2005, in prep.
 Buccheri, R., et al. 1983, *A&A*, 128, 245
 Camilo, F., Manchester, R. N., Gaensler, B. M., & Lorimer, D. R. 2002, *ApJ*, 579, L25
 Dame, T. M., Hartmann, D., & Thaddeus, P. 2001, *ApJ*, 547, 792
 Dickey, J. M., & Lockman, F. J. 1990, *ARA&A*, 28, 215
 Fich, M., Blitz, L., & Stark, A. A. 1989, *ApJ*, 342, 272
 Gardner, F. F., Whiteoak, J. B., & Otrupcek, R. E. 1983, *Proceedings of the Astronomical Society of Australia*, 5, 221
 Green, D. A. 2004, *Bull. Astro. Soc. India*, 32, 335
 Gotthelf, E. V., Ueda, Y., Fujimoto, R., Kii, T., & Yamaoka, K. 2000, *ApJ*, 543, 417
 Handa, T., Sofue, Y., Nakai, N., Hirabayashi, H., & Inoue, M. 1987, *PASJ*, 39, 709
 Haynes, R. F., Caswell, J. L., & Simons, L. W. J. 1978, *Australian Journal of Physics Astrophysical Supplement*, 45, 1
 Hendrick, S. P., & Reynolds, S. P. 2001, *ApJ*, 559, 903
 Kaspi, V. M. and Roberts, M. S. E. and Harding, A. K. 2005, in *Compact Stellar X-ray Sources*, eds. Lewin, W. H. G. & van der Klis, M., CUP Cambridge, in press, astro-ph/0402136
 Kassim, N. E. 1989, *ApJ*, 347, 915
 Lazentic, J. S., Slane, P. O., Gaensler, B. M., Reynolds, S. P., Plucinsky, P. P., & Hughes, J. P. 2004, *ApJ*, 602, 271
 Malkov, M. A., Diamond, P. H., & Sagdeev, R. Z. 2005, *ApJ*, 624, L37
 Manchester, R. N., et al. 2001, *MNRAS*, 328, 17
 Manchester, R. N., Hobbs, G. B., Teoh, A., & Hobbs, M. 2005, *AJ*, 129, 1993
 McClure-Griffiths, et. al. 2005, *ApJS*, in press, astro-ph/0503134
 Pohl, M. 2001, “27th International Cosmic Ray Conference” ed. Schlickeiser, R., Copernicus Group, astro-ph/0111552
 Possenti, A., Cerutti, R., Colpi, M., & Mereghetti, S. 2002, *A&A*, 387, 993
 Radhakrishnan, V., Goss, W. M., Murray, J. D., & Brooks, J. W. 1972, *ApJS*, 24, 49
 Reich, W., Reich, P., & Fuerst, E. 1990, *A&AS*, 83, 539
 Reynolds, S. P. 1996, *ApJ*, 459, L13
 Reynolds, S. P., & Keohane, J. W. 1999, *ApJ*, 525, 368
 Sato, F. 1977, *PASJ*, 29, 75
 Sedov, L. I. 1959, *Similarity and Dimensional Methods in Mechanics*, New York: Academic Press, 1959
 Uchiyama, Y., Aharonian, F. A., Takahashi, T., Hiraga, J. S., Moriguchi, Y., & Fukui, Y. 2005, *AIP Conf. Proc.* 745: High Energy Gamma-Ray Astronomy, 745, 305

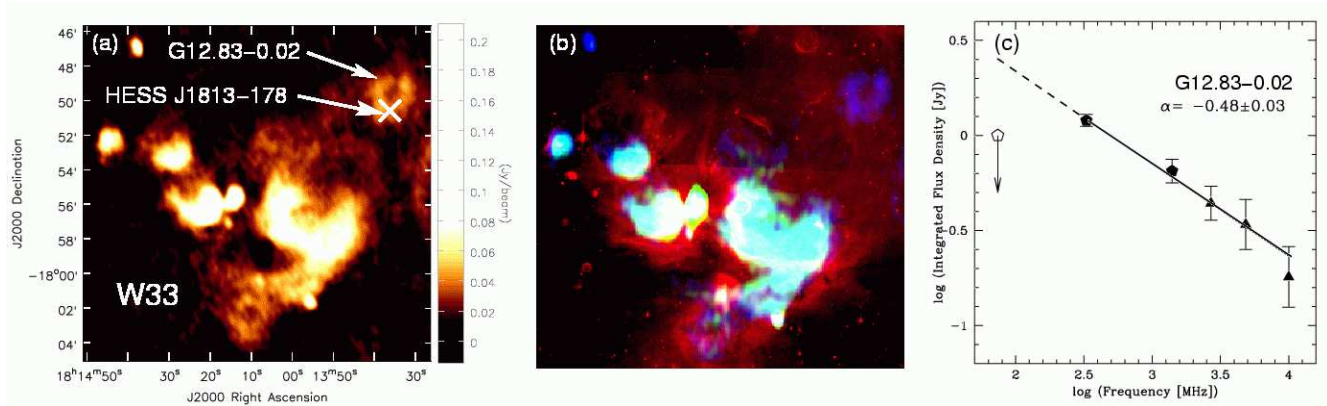


FIG. 1.— (a) VLA 90cm image of G12.82–0.02 with $32'' \times 19''$ resolution. The cross indicates the position of HESS J1813–178 which has a positional uncertainty of $1''-2''$ (Aharonian et al. 2005a). (b) Three color image of the same region as (a), with red=*Spitzer* 8 μm , green=VLA 20cm, and blue=VLA 90cm. Thermal emission is white to cyan or red in color, while non-thermal emission is darker blue. (c) Radio spectrum for SNR G12.8–0.0. Solid hexagon symbols are from the current work at 20 and 90cm. The open hexagon symbol indicates the 5–4m upper limit. The N symbols indicate flux densities from the 11cm Bonn, 6cm Parkes, and 3cm Nobeyama single dish surveys (Reich, Reich, & Fuerst 1990; Haynes et al. 1978; Handa et al. 1987). The line (solid and dashed) shows a power-law weighted least squares fit to the radio data for 330 MHz (90cm).

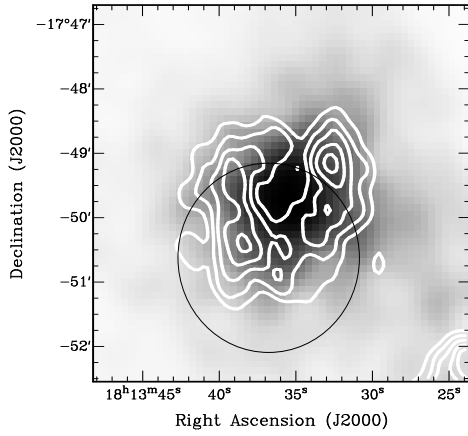


FIG. 2.— ASCA SIS greyscale image of AX J1813–178 in the energy range 0.5–10 keV smoothed to $30''$ with 90cm contours at 28, 33, 38, 43, and 48 mJy beam^{-1} overlaid (contour intervals are 2 mJy beam^{-1}). The resolution of the 90cm data is $32'' \times 19''$. The black circle indicates the position and angular extent ($3''$) of HESS J1813–178.

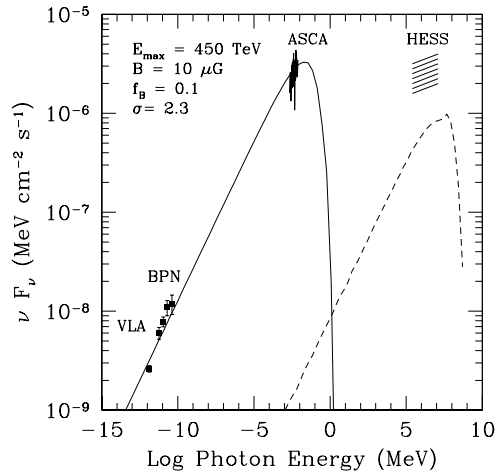


FIG. 3.— Fit to the broadband emission assuming that all the flux originates from the shell of SNR G12.8–0.0. The model includes contributions from synchrotron (solid line) and IC (dashed line) mechanisms. BPN stands for Bonn, Parkes, and Nobeyama. We have assumed a typical SNR magnetic field strength $B = 10 \text{ G}$ and that the field occupies 10% of the IC emitting region (i.e. $f_B = 0.1$). Our fitted electron spectral index ($\alpha = 2.3$) is consistent with that expected for first order Fermi acceleration. The diagonal lines indicate both the uncertainty in the HESS flux measurements, and the fact that no spectral information has yet been published for the TeV emission (Aharonian et al. 2005a).